Chinese Chemical Letters 34 (2023) 107559

Contents lists available at ScienceDirect

Chinese Chemical Letters

journal homepage: www.elsevier.com/locate/cclet

Frustrated Lewis pairs *in situ* formation in B-based porous aromatic frameworks for efficient *o*-phenylenediamine cyclization

Anqi Dai[1], Shulin Li[1], Tienan Wang, Yuting Yang, Yuyang Tian, Xiaofei Jing*, Guangshan Zhu

Key Laboratory of Polyoxometalate and Reticular Material Chemistry of Ministry of Education, Faculty of Chemistry, Northeast Normal University, Changchun 130024, China

ARTICLE INFO

Article history:
Received 25 April 2022
Revised 22 May 2022
Accepted 24 May 2022
Available online 28 May 2022

Keywords:
Porous aromatic frameworks (PAFs)
Co_2 capture and conversion
Gas sorption
Frustrated lewis pairs (FLPs)
Heterogeneous catalysis

ABSTRACT

Benzimidazoles are very important chemical materials in the pharmaceutical industry, and the most common synthetic route is cyclization of *o*-phenylenediamine with carbon sources, in which utilization of inexpensive and abundant CO_2 as C1 source is very impressive. Porous aromatic frameworks (PAFs) with highly desired skeletons have attracted great attentions in gas capture and catalysis. Herein, B-based PAF-165 and PAF-166 are designed and synthesized *via* Friedel-Crafts alkylation reaction, which present high surface areas as well as high stability. Benefiting from the abundant electron-deficient B centers, both PAFs exhibit excellent selective CO_2 adsorption abilities. The presence of sterically hindered B units in PAFs can act as Lewis acid active sites for the frustrated Lewis pairs (FLPs) *in situ* formation with *o*-phenylenediamine, thus promoting the synthesis of benzimidazole. The optimal reaction conditions for *o*-phenylenediamine cyclization with PAF catalysts are explored, and the reaction mechanism is also proposed. This work provides feasible ideas for incorporating FLPs within porous materials as reusable heterogeneous catalysts for CO_2 capture and conversion.

Carbon dioxide (CO_2) is a typical greenhouse gas, and its amount in the atmosphere has been on continuous rise because of the large-scale combustion of fossil fuels [1,2]. Meanwhile, CO_2 is an ideal renewable and nontoxic carbon source in chemical synthesis [3,4]. CO_2 capture and conversion strategy, which can not only reduce its adverse impact on the environment but also produce high value-added chemical products, has attracted great attentions and become a hot topic [5–7]. Benzimidazoles are widely used to synthesize many kinds of natural products and bioactive molecules, such as mebendazole [8], omeprazole [9], albendazole [10] and pantoprazole [11]. The most common synthetic route for benzimidazoles is direct synthesis from *o*-phenylenediamine with carbon sources, in which utilization of inexpensive and abundant CO_2 as C1 source is very impressive. However, CO_2 is a relatively stable molecule, so highly efficient catalysts are needed in this approach.

Frustrated Lewis pairs (FLPs) formed by the steric resistance of Lewis acids and bases have aroused significant attentions due to their highly efficient catalytic activities in non-metal-mediated catalysis [12–15]. Currently, FLPs are well investigated for small-molecule activation, such as H_2 [16,17] and CO_2 [18,19]. Chen *et al.* synthesized two copolymers installing bulky borane- and phosphine-containing blocks respectively and built them as the macromolecular FLP which can effectively bound CO_2 and then serve as recyclable catalysts [19]. Usually, homogeneous FLP catalysts encounter separation difficulty from the reaction system thus resulting in poor catalyst recycle [20]. In order to solve this problem, FLPs combined with solid materials to form heterogeneous catalysts are explored [21,22]. Shyshkanov *et al.* reported a water-stable and recyclable MOF catalyst contained Lewis acidic sites (B centers) for the synthesis of benzimidazoles from *o*-phenylenediamine under CO_2 atmosphere by the *in situ* formation of FLPs [23]. This proves that utilizing porous materials incorporating Lewis acidic centers would create FLPs during synthesis of benzimidazoles with CO_2, which would act as promising heterogeneous catalysts.

Porous aromatic frameworks (PAFs) have been developed as a novel class of porous materials due to their robust skeletons and high surface areas [24]. Benefiting from the variety of synthesis and functionalization, it is possible to customize specific properties in PAF skeletons, which provides great opportunities for their applications in gas adsorption [25–27], separation [28,29], sen-

* Corresponding author.
E-mail address: jingxf100@nenu.edu.cn (X. Jing).
[1] These authors contributed equally to this work.

https://doi.org/10.1016/j.cclet.2022.05.073
1001-8417/

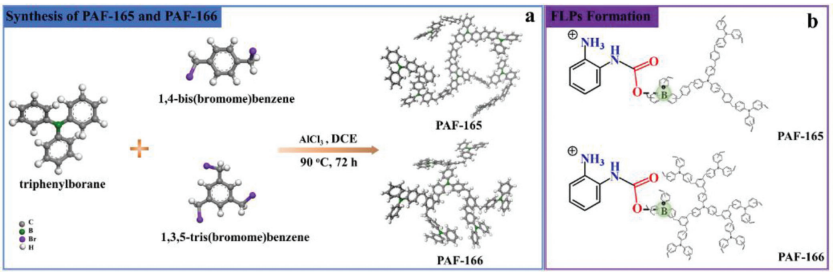

Scheme 1. The synthetic routes of (a) PAF-165 and PAF-166 and (b) FLPs *in situ* formation with *o*-phenylenediamine .

sors [30–32], heterogeneous catalysis [33,34] and so on. Thomas group synthesized triphenylphosphine-based porous networks to mimic the basic sites employed in FLPs [35]. N-rich PAF-6 with layer structure was exfoliated into nanosheets to reveal its featured Lewis base sites and then served as heterogeneous FLP catalyst by interacting with the strong Lewis acid $B(C_6F_5)_3$ [36]. Therefore, by virtue of the structural advantages of PAFs, introducing sterically encumbered B, P and N motifs would produce potential Lewis acid and base groups to achieve post-decorated FLPs, which are effective heterogeneous FLP catalysts for H_2 and CO_2 activation. Herein, a sterically hindered B motif (triphenylboron) was selected as building units and two B-based PAFs (PAF-165 and PAF-166) were synthesized *via* Friedel-Crafts alkylation. Both PAFs possess high surface areas (867 m^2/g for PAF-165 and 754 m^2/g for PAF-166) together with high thermal stabilities. Due to the presence of electron-deficient B centers, these PAFs exhibited highly enhanced CO_2 adsorption abilities and selective adsorption over N_2. At 273 K and 1 bar, the equimolar mixture selectivities of PAF-165 and PAF-166 estimated with the ideal adsorbed solution theory (IAST) are 106.2 and 196.5, respectively. Additionally, PAF-165 and PAF-166 showed excellent catalytic abilities in the synthesis of benzimidazole from *o*-phenylenediamine with CO_2 source, in which triphenylboron units in PAFs acted as Lewis acid sites and form FLPs catalyst with substrates during the reaction.

As illustrated in Scheme 1, PAF-165 and PAF-166 were synthesized *via* Friedel-Crafts alkylation reaction between triphenylboron and Br-substituted external cross-linkers (1,4-bis(bromomethyl)benzene or 1,3,5-tris(bromomethyl)benzene). Both PAFs contain abundant Lewis acid active sites for the *in situ* formation of FLPs upon addition of *o*-phenylenediamine.

Comparative FTIR spectra of PAF-165, PAF-166 and their corresponding monomers were collected to confirm the bonding features in their frameworks (Fig. S1 in Supporting information). The peaks at 1600 and 1460 cm^{-1} ascribed to benzene rings are retained after reaction. The absence of C-Br characteristic bands at 610 and 580 cm^{-1} along with the appearance of stretching vibrations at 2930 cm^{-1} for methylene group reveal that polymerization reaction completed successfully. To further illustrate the local structures of PAF-165 and PAF-166, solid-state ^{13}C MAS NMR and ^{11}B MAS NMR were performed [37]. As shown in Fig. S2a (Supporting information), the signals at 137 and 131 ppm are clearly observed, which are attributed to substituted and unsubstituted phenyl carbons in PAF skeletons, respectively. The signals at 32 and 15 ppm can be assigned to methylene linkers and methylene end groups, indicating that the Br-substituted external cross-linkers have participated the polymerization process. There is only one peak in ^{11}B MAS NMR spectra of as-synthesized PAFs (Fig. S2b in Supporting information, 16.3 ppm for PAF-165 and 19.1 ppm for PAF-166), suggesting that boron centers are successfully introduced in PAFs skeletons without changes of connection ways. PXRD were then employed to explore the long-range order of resulted PAFs, and no obvious diffraction peak is observed (Fig. S3 in Supporting information), confirming disordered PAF structures which is common in the dynamic-driven irreversible reactions. SEM images (Figs. S4a and b in Supporting information) showed that both PAFs are well-defined spherical particles, while TEM images (Figs. S4c and d in Supporting information) indicated that these two PAFs possess worm-like porous textures. TGA curves (Fig. S5 in Supporting information) were collected to investigate PAFs' stabilities which show that both PAF-165 and PAF-166 are stable up to 350 °C in air condition. In addition, they cannot be dissolved in various solvents such as methanol, ethanol, dichloromethane, toluene, acetone, HCl solution (3 mol/L) and other common organic solvents. These results suggest that the resulted PAFs have high thermal stability together with high chemical stability. This is in favor of the recyclability of catalysts and plays an important role in heterogeneous catalytic systems [33].

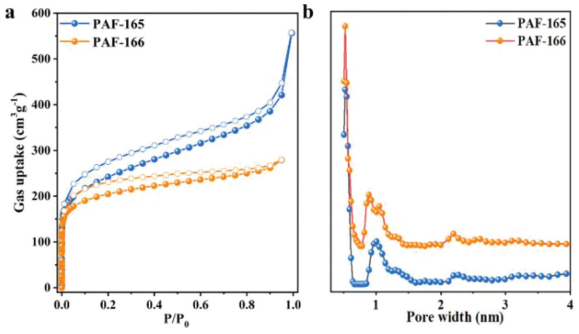

Fig. 1. (a) N_2 adsorption-desorption isotherms at 77 K and (b) the pore size distributions calculated from NLDFT for PAF-165 and PAF-166.

In order to investigate the porosity of PAF-165 and PAF-166, N_2 adsorption-desorption measurements were carried out at 77 K. As shown in Fig. 1a, the adsorption capacities of PAFs increase sharply in the relative low-pressure region ($P/P_0 < 0.01$) and hysteresis loops between the adsorption and desorption curves are observed, which suggest the presence of micropores and mesopores in their frameworks [27]. According to Brunauer-Emmett-Teller (BET) model, PAF-165 and PAF-166 present high surface areas of 867 and 754 m^2/g, respectively. Meanwhile, their pore size distributions were calculated based on the nonlocal density functional theory (NLDFT), and provid two main pores around 0.5 and 1 nm as well as a few distributions at 2.2 nm (Fig. 1b), consistent with the results form sorption isotherms. The pore volumes of PAF-165 and PAF-166 were calculated to be 0.70 and 0.41 cm^3/g, respectively. The high surface areas together with uniform porous textures of PAFs would provide enough space for the formation of FLPs and facilitate timely separation of reactants and products during catalytic process.

Given the highly porous frameworks and abundant B centers as Lewis acid sites in PAF-165 and PAF-166, CO_2 adsorption measurements were conducted to explore PAFs' binding abilities to CO_2 molecules. CO_2 adsorption isotherms at 273 and 298 K were col-

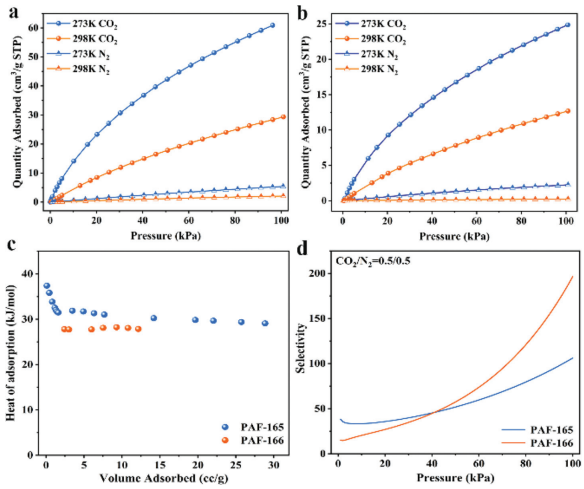

Fig. 2. CO_2 and N_2 adsorption isotherms of (a) PAF-165 and (b) PAF-166 at 273 and 298 K, respectively. (c) Q_{st} of CO_2 and (d) IAST-predicted adsorption selectivity of equimolar CO_2 and N_2 at 273 K for PAF-165 and PAF-166.

lected for each PAFs, while N_2 adsorption under the same conditions were also carried out for comparison. As illustrated in Figs. 2a and b, both PAF-165 and PAF-166 exhibit obvious differences on CO_2 and N_2 adsorption. As the pressure increases, the adsorption capacities of CO_2 raise correspondingly, whereas N_2 adsorption capacities show negligible changes. This suggests that both PAFs possess greater affinity for CO_2 than N_2. At 273 K and 1 bar, PAF-165 possesses higher CO_2 uptake (60.90 cm^3/g) than PAF-166 (24.88 cm^3/g), which is probably due to its higher surface area and lager pore volume (Table S1 in Supporting information). To further evaluate CO_2 affinity with PAFs, the isosteric heats of adsorption (Q_{st}) were calculated using the Clausius-Clapeyron equation [38]. At zero loading, Q_{st} of CO_2 are 37.4 and 27.8 kJ/mol for PAF-165 and PAF-166, respectively (Fig. 2c), higher than may reported porous materials such as PAF-18-OLi (29 kJ/mol) [27], PAF-26-COOK (32.6 kJ/mol) [29], Cu-BTC (30 kJ/mol) [39] and HCP-CN (26.9 kJ/mol) [40]. In addition, the well-developed ideal solution adsorbed theory (IAST) was employed to predict the CO_2/N_2 selectivity. Firstly, CO_2 and N_2 adsorption isotherms of PAF-165 and PAF-166 at 273 K were fitted by using the dual-site Langmuir Freundlich (DSLF) equation, which give well-fitted isotherms for both PAFs (Fig. S6 in Supporting information). The calculated selectivities of equimolar CO_2 over N_2 273 K are 33.8 for PAF-165 and 14.9 for PAF-166 at a pressure of 1.05 kPa (Fig. 2d), confirming their stronger CO_2 capture abilities.

As described above, PAF-165 and PAF-166 with high surface areas along with uniform pore size distributions were synthesized successfully. Benefiting from the presence of electron-deficient B centers, these two PAFs exhibit great selective adsorption abilities for CO_2. The sterically hindered B building units could act as Lewis acid sites and take part in the *in situ* formation of FLPs with *o*-phenylenediamine, which will become efficient catalysts for CO_2 activation and promote the synthesis of benzimidazoles. Compared to PAF-166, PAF-165 has higher surface area and larger pore volume, which is more favorable for the mass transfer process, so PAF-165 was firstly used to explore the optimal reaction conditions for the synthesis of benzimidazole from *o*-phenylenediamine, where CO_2 was utilized as a C1 source. The type and amount of reducing agents, reaction temperatures, solvents and reaction times were fully investigated. The catalytic products were analyzed by GC–MS, in which diphenyl was used as internal standard and 2-methylbenzimidazole was determined to be the only by-product (Fig. S7 and Table S2 in Supporting information). First

Table 1
Optimization of reaction conditions for the synthesis of benzimidazoles from *o*-phenylenediamine.[a]

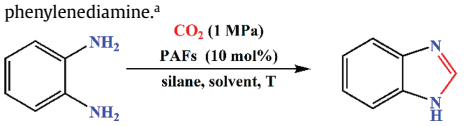

Entry	Hydrosilane (equiv.)	Temp. (°C)	Solvent	Conv. (%)	Sel. (%)
1	Ph_2SiH_2 (4)	100	THF	33	32
2	Ph_2SiH_2 (4)	120	THF	51	73
3	Ph_2SiH_2 (4)	140	THF	47	77
4	$PhSiH_3$ (4)	100	THF	>99	99
5	$PhSiH_3$ (4)	120	THF	>99	98
6	$PhSiH_3$ (4)	140	THF	99	97
7	$PhSiH_3$ (4)	120	DMSO	>99	42
8	$PhSiH_3$ (4)	120	ACN	>99	50
9	Ph_2SiH_2 (4)	120	ACN	92	87
10[b]	$PhSiH_3$ (4)	120	THF	30	76
11	$PhSiH_3$ (2)	120	THF	44	97
12[c]	$PhSiH_3$ (4)	120	THF	>99	89
13[c]	$PhSiH_3$ (4)	120	ACN	>99	95
14[d]	$PhSiH_3$ (4)	120	THF	trace	trace

[a] Reactions were carried out in PTFE-lined autoclaves with *o*-phenylenediamine (0.4 mmol), silane (1.6 mmol) and PAF-165 (10 mol%) in 4 mL of solvent in CO_2 (1.0 MPa) atmosphere, reaction time: 24 h.
[b] Reaction time: 12 h.
[c] Catalyst: PAF-166 (10 mol%).
[d] No catalyst.

of all, two reducing agents, diphenylsilane (Ph_2SiH_2) and phenyl silane ($PhSiH_3$) were chosen and the reactions were carried out in tetrahydrofuran (THF) at different temperatures including 100, 120 and 140 °C for 24 h. It shows that the conversion and selectivity in Ph_2SiH_2 reduced reactions (Table 1, entries 1–3) are at low levels, while $PhSiH_3$ involved reactions obtain high conversions (>99%) together with selectivities above 97% (Table 1, entries 4–6) at all temperatures. Then, another two solvents including dimethyl sulfoxide (DMSO) and acetonitrile (ACN) were tried. Although high conversions (>99%) are achieved, the selectivities are only up to 50% (Table 1, entries 7 and 8). Ph_2SiH_2 was also tested in ACN system, and the conversion is higher than that in THF, but the selectivity is still not good enough (Table 1, entry 9). After that, the reaction time was reduced to 12 h (Table 1, entry 10) and dosage of $PhSiH_3$ was cut down by 50% (Table 1, entry 11), respectively, whereas both conversions and selectivities decreased. Therefore, the optimal cyclization reaction proceeds in THF system under the reduced effect of $PhSiH_3$ (4 equiv.) for 24 h. PAF-166 was utilized to verify its catalytic activity using the above condition, and conversion greater than 99% is obtained (Table 1, entry 12). ACN system was also tried with PAF-166, which accomplishes high conversion (>99%, Table 1, entry 13). Under the same optimized reaction condition, conversions of >99% are obtained in both PAF-165 and PAF-166 catalyzed systems (Table 1, entries 5 and 12), whereas selectivity is higher in the reaction catalyzed by PAF-165. This might be attributed to the higher surface area and larger pore volume of PAF-165, which can provide more effective contact areas for the formation of FLPs with *o*-phenylenediamine and is also beneficial for the separation of reactants and products. Furthermore, the cyclization of *o*-phenylenediamine was conducted without the addition of PAF catalysts (Table 1, entry 14), and only trace benzimidazole was detected by GC–MS analysis, proving the critical role of PAF catalysts in this reaction. Their catalytic performances are comparable with many other catalysts, such as SION-105, Rh@PS, Au/TiO_2 (Table S3 in Supporting information).

Considering economic cost and environmental friendliness, the recyclability of PAF catalysts was also investigated. PAF-165 and PAF-166 with distinguished thermal and chemical stability can be easily separated from the reaction system *via* filtration or centrifu-

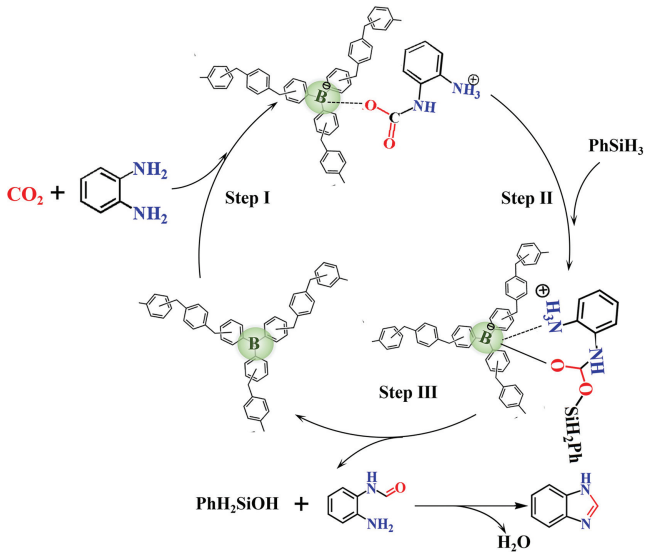

Fig. 3. Proposed reaction mechanism for the cyclization of *o*-phenylenediamine catalyzed by PAF-165.

gation. After being washed with dichloromethane and methanol thoroughly and then dried under vacuum for 6 h, these PAFs were used in the next cycle. After five successful cycles, the conversions of *o*-phenylenediamine cyclization under the optimal reaction conditions reach up to 99% for PAF-165 and 92% for PAF-166 (Fig. S8 in Supporting information). The structural features of recycled PAFs were studied with FTIR (Fig. S9 in Supporting information), SEM (Fig. S10 in Supporting information) and TGA (Fig. S11 in Supporting information), respectively. All the results are in good agreements with the fresh PAFs catalysts, indicating their excellent recyclability.

Furthermore, the reaction mechanism of PAFs catalyzed *o*-phenylenediamine cyclization *via in situ* formation of FLPs with sterically hindered B units in PAFs and *o*-phenylenediamine substrates were speculated based on the previous reported methods [19,23]. As illustrated in Fig. 3, B center in PAFs and N atom of *o*-phenylenediamine react with CO_2 molecule to form CO_2 adduct in step I. Then, Si atom in the reducing agent $PhSiH_3$ connects with one O atom in CO_2 adduct (step II), and subsequently PhH_2SiOH releases from the reaction to give out *N*-(2-aminophenyl)formamide (step III), which produces the final product 1*H*-1,3-benzodiazole by dehydration reaction (step IV).

In summary, by selecting triphenylboron as building units, two novel B-based PAFs, PAF-165 and PAF-166, are successfully synthesized *via* Friedel-Crafts alkylation reaction. Profiting from the highly porous frameworks, uniform pore size distributions and the presence of electron-deficient B centers, PAF-165 and PAF-166 exhibit great CO_2 adsorption capacity as well as highly selective CO_2 adsorption abilities over N_2. Because B centers are sterically hindered in resultant PAFs, they act as Lewis acid sites and combine with Lewis basis substrates (*o*-phenylenediamine) to *in situ* form FLPs, which present effectively catalytic performance in the synthesis of benzimidazole from *o*-phenylenediamine, where CO_2 is utilized as a C1 source. Meanwhile, the reaction mechanism of *o*-phenylenediamine cyclization catalyzed by B-based PAFs is speculated to better understand the relationship of PAFs structures and catalytic activity. This work offers a promising strategy for developing FLPs-involved porous materials as heterogeneous catalysts for the synthesis of benzimidazoles, which also is an effective way for CO_2 capture and conversion.

Declaration of competing interest

The authors declare that they have no known competing financial interests or personal relationships that could have appeared to influence the work reported in this paper.

Acknowledgments

We are grateful for the financial support by the Fundamental Research Funds for the Central Universities (No. 2412019FZ008), the National Natural Science Foundation of China (Nos. 22131004 and U21A20330) and the "111″ Project (No. B18012).

Supplementary materials

Supplementary material associated with this article can be found, in the online version, at doi:10.1016/j.cclet.2022.05.073.

References

[1] D.H. Nam, P. De Luna, A. Rosas-Hernandez, et al., Nat. Mater. 19 (2020) 266–276.
[2] P. Gao, L. Zhang, S. Li, Z. Zhou, Y. Sun, ACS Cent. Sci. 6 (2020) 1657–1670.
[3] H. Gu, L. Zhong, G. Shi, et al., J. Am. Chem. Soc. 143 (2021) 8679–8688.
[4] S. Mukhopadhyay, R. Shimoni, I. Liberman, et al., Angew. Chem. Int. Ed. 60 (2021) 13423–13429.
[5] Z. Yang, B. Yu, H. Zhang, et al., ACS Catal. 6 (2016) 1268–1273.
[6] J. Liu, C. Chen, K. Zhang, L. Zhang, Chin. Chem. Lett. 32 (2021) 649–659.
[7] L.H. Han, J.Y. Li, Q.W. Song, et al., Chin. Chem. Lett. 31 (2020) 341–344.
[8] Y.L. Li, D. Thomas, A. Deutzmann, et al., Sci. Rep. 9 (2019) 16775–16783.
[9] M. Gilard, B. Arnaud, J.C. Cornily, et al., J. Am. Coll. Cardiol. 51 (2008) 256–260.
[10] L. Prchal, R. Podlipna, J. Lamka, et al., Environ. Sci. Pollut. Res. Int. 23 (2016) 13015–13022.
[11] K. Takeuchi, A. Konaka, M. Nishijima, S. Kato, T. Yasuhiro, J. Gastroenterol. Hepatol. 14 (1999) 251–257.
[12] D.W. Stephan, Science 354 (2016) aaf7229.
[13] D.J. Scott, T.R. Simmons, E.J. Lawrence, et al., ACS Catal. 5 (2015) 5540–5544.
[14] J. Lam, K.M. Szkop, E. Mosaferi, D.W. Stephan, Chem. Soc. Rev. 48 (2019) 3592–3612.
[15] D.J. Scott, M.J. Fuchter, A.E. Ashley, Angew. Chem. Int. Ed. 53 (2014) 10218–10222.
[16] A. Willms, H. Schumacher, T. Tabassum, et al., Chem. Commun. 10 (2018) 1835–1843.
[17] S. Mummadi, A. Brar, G. Wang, et al., Chemistry 24 (2018) 16526–16531 (Easton).
[18] S. Zhang, Z.M. Xia, Y. Zou, et al., J. Am. Chem. Soc. 141 (2019) 11353–11357.
[19] L. Chen, R.J. Liu, Q. Yan, Angew. Chem. Int. Ed. 57 (2018) 9336–9340.
[20] F.W. Ding, Y.L. Zhang, R. Zhao, et al., Chem. Commun. 53 (2017) 9262–9264.
[21] A. Willms, H. Schumacher, T. Tabassum, et al., ChemCatChem 10 (2018) 1835–1843.
[22] Z. Niu, W. Zhang, P.C. Lan, B. Aguila, S. Ma, Angew. Chem. Int. Ed. 58 (2019) 7420–7424.
[23] S. Shyshkanov, T.N. Nguyen, F.M. Ebrahim, K.C. Stylianou, P.J. Dyson, Angew. Chem. Int. Ed. 58 (2019) 1–6.
[24] Y. Tian, G. Zhu, Chem. Rev. 120 (2020) 8934–8986.
[25] T. Ben, H. Ren, S.Q. Ma, et al., Angew. Chem. Int. Ed. 48 (2009) 9457–9460.
[26] Z.J. Yan, H. Ren, H.P. Ma, et al., Microporous Mesoporous Mater. 173 (2013) 92–98.
[27] H. Ma, H. Ren, X. Zou, et al., J. Mater. Chem. A 1 (2013) 752–758.
[28] L. Jiang, Y. Tian, T. Sun, et al., J. Am. Chem. Soc. 140 (2018) 15724–15730.
[29] H. Ma, H. Ren, X. Zou, et al., Polym. Chem. 5 (2014) 144–152.
[30] H. Ma, B. Li, L. Zhang, D. Han, G. Zhu, J. Mater. Chem. A 3 (2015) 19346–19352.
[31] T. Ma, X. Zhao, Y. Matsuo, et al., J. Mater. Chem. C 7 (2019) 2327–2332.
[32] A.T. Vilian, P. Puthiaraj, C.H. Kwak, et al., ACS Appl. Mater. Interfaces 8 (2016) 12740–12747.
[33] Y.T. Yang, T.N. Wang, X.F. Jing, G.S. Zhu, J. Mater. Chem. A 7 (2019) 10004–10009.
[34] L.P. Jing, J.S. Sun, F. Sun, P. Chen, G. Zhu, Chem. Sci. 9 (2018) 3523–3530.
[35] M. Trunk, J.F. Teichert, A. Thomas, J. Am. Chem. Soc. 139 (2017) 3615–3618.
[36] Q. Meng, Y. Huang, D. Deng, et al., Adv. Sci. 7 (2020) 2000067.
[37] Y. Yang, Y. Yang, T. Wang, et al., Microporous Mesoporous Mater. 306 (2020) 110393–110340.
[38] H. He, F. Sun, B. Aguila, et al., J. Mater. Chem. A 4 (2016) 15240–15246.
[39] Z. Liang, M. Marshall, A.L. Chaffee, Energy Procedia 1 (2009) 1265–1271.
[40] Y. Cheng, S. Razzaque, Z. Zhan, B. Tan, Chem. Eng. J. 426 (2021) 130731.